A Low-Power DWS-CNN-Based Downsampling Approach for Odor Identification Using Herbal and Organic Datasets

Akshata K. Aldi
Department of Applied Electronics, Gulbarga University, Kalaburagi, Karnataka, India
akshatakaldi@gmail.com (corresponding author)

R. L. Raibagkar
Department of Applied Electronics, Gulbarga University, Kalaburagi, Karnataka, India
raibagkarrl@gmail.com

Received: 14 February 2026 | Revised: 2 April 2026 and 23 April 2026 | Accepted: 30 April 2026

 DOI: https://doi.org/10.48084/etasr.18175

ABSTRACT

Odor identification systems play an important role in food safety applications, herbal authentication, and portable sensing devices. These systems help identify the essential properties of natural organic substances with fast processing speed, low power consumption, and high accuracy. Traditional odor analysis methods provide precise detection and structured gas sensor measurements, yet they involve high computational cost, large architectures, slow data inference, and limited suitability for FPGA- and embedded system-based real-time applications. Furthermore, traditional Convolutional Neural Network (CNN) architectures generally require multiple convolutional layers, large memory resources, high hardware utilization, and increased classification latency, making them unsuitable for low-power applications such as odor identification and character recognition. Therefore, the proposed Depthwise Separable Convolutional Neural Network (DWS-CNN) was specifically developed for low-power applications using a 26×26 input window size. The proposed architecture acquires 676 samples every 65.36 µs at a frequency of 100 MHz. In addition, it classifies odor identification data from various herbal and organic datasets using multiclass dense classification with a 3×3 window size. The proposed model simultaneously predicts and classifies 12 different sensing values from 50 distinct categories. The entire architecture was implemented in Verilog HDL and functionally verified using Modelsim. The design was synthesized on an Artix-7 FPGA, achieving a low power consumption of 0.362 W and a latency of 4.146 ns, demonstrating its suitability for real-time odor identification applications.

Keywords-odor identification; multiclass dense classification; Convolutional Neural Network (CNN); herbal and organic datasets

I. INTRODUCTION

Odor identification has become an important technology in modern sensing applications, especially in food safety, herbal authentication, environmental monitoring, industrial quality inspection, and portable healthcare systems [1-3]. These applications depend on the accurate detection of Volatile Organic Compounds (VOCs), where electronic nose platforms mimic human olfactory perception using combinations of gas sensors [4-7]. Compared to traditional chemical laboratory methods, electronic nose systems are compact, inexpensive, and capable of operating continuously without specialized equipment [8]. Their ability to transform complex gas signatures into measurable electronic patterns makes them suitable for handheld devices with the help of the Internet of Things (IoT) platform and embedded monitoring systems [1, 9].

However, Convolutional Neural Network (CNN) architectures with numerous convolution and pooling layers, deeper networks, wide filter sizes, and fully connected layers generally result in higher inference time and computational cost [10, 11]. In odor analysis, gas sensors exhibit slower chemical dynamics, cross-sensitivity, and environmental dependency, requiring algorithms that process large segments of temporal data [12, 13]. As a result, real-time classification becomes challenging, especially when the number of odor categories increases [14, 15]. Many existing odor classification approaches rely on deep CNNs with high computational complexity and large memory requirements, making them

unsuitable for low-power embedded platforms such as FPGA-based electronic nose systems [16]. This limitation represents the primary motivation for the present research. Furthermore, traditional odor identification systems rely on one-dimensional CNN (1D-CNN) or deep two-dimensional CNN (2D-CNN) frameworks with thousands of parameters, which require significant hardware resources for practical deployment [17-19]. Recent studies have shown that Depthwise Separable Convolutional Neural Networks (DWS-CNNs) can significantly reduce model complexity while preserving classification performance in resource-constrained applications [20]. Hence, a lightweight and low-power odor identification system capable of classifying natural organic and herbal substances was designed using a minimal set of sensing inputs, reduced computational complexity, and a hardware-friendly CNN architecture.

A DWS-CNN is specifically designed for low power odor identification [19]. This system uses a compact 26×26 input representation derived from odor sensor datasets and applies depthwise convolution, pointwise convolution, and max-pooling to downsample the data [21]. By compressing the spatial dimension from 26×26 to a 3×3 window, the model removes unnecessary operations while preserving essential features from the 12 sensing channels. This approach eliminates heavy convolution blocks and reduces the reliance on large fully connected layers. Furthermore, the classification stage uses a compact multiclass dense layer on a 72-bit flattened vector, enabling fast hardware execution.

The proposed architecture is carefully structured to ensure low computational cost, reduced memory transactions, and compatibility with FPGA design methodologies. The novelty of this work lies in the design of a low-power depthwise CNN-based downsampling approach tailored for odor identification of natural organic substances [22]. Traditional CNNs employ wide filters and deep layers with extensive kernel multiplications, whereas the proposed model reduces the number of layers and kernel multiplications and adopts an efficient hierarchical max-pooling approach to reduce the feature size from 26×26 to 3×3. Additionally, this design minimizes line buffer usage, using First-In First-Out (FIFO) memory operations for efficient kernel multiplication and max-pooling processing [23]. This design reduces the number of convolution operations and ensures a balanced implementation that fits the constraints of modern low-cost FPGAs [24]. The proposed method extends beyond conventional VOC or herbal medicine detection by classifying a wide range of natural organic categories [25]. Compared to previously reported studies, this model achieves faster inference time, controlled hardware utilization, lower power consumption, and minimal latency for real-time processing of multidimensional sensor inputs, contributing to a practical solution for handheld, portable, and embedded odor classification systems [26].

II. EXPERIMENTAL DESIGN AND ARCHITECTURE

This proposed odor identification system employs a lightweight DWS-CNN specifically designed for low-power hardware execution on FPGA devices [17]. The novelty of this work lies in operating the CNN with a compact 26×26 window size, which takes input from odor sensor datasets and extracts spatial odor features using an energy-efficient convolution mechanism. In contrast to conventional CNNs that apply a full 3×3 kernel across all channels, the proposed CNN architecture separates spatial filtering and channel projection into depthwise and pointwise convolutions. This method significantly reduces the number of multiplications, memory transfers, and intermediate feature computations, making the architecture suitable for real-time embedded odor analysis.

By using multisensory gas sensor analysis for odor identification, 12 sensing parameters were included for chemical gas indices such as NO_2, C_2H_5OH, VOC, CO, alcohol, LPG, benzene, and environmental factors such as temperature, pressure, humidity, gas resistance, and altitude. Each parameter is processed through an independent 26×26 CNN, where the feature map is gradually reduced from 24×24 to 12×12, 6×6, and finally 3×3 through depthwise convolutions supported by large 6×6 max-pooling operations. The use of large max-pooling windows enables aggressive spatial compression with minimal computational cost while preserving dominant odor signatures. The Rectified Linear Unit (ReLU) activation function ensures nonlinearity, numerical simplicity, and supports FPGA-friendly fixed-point data paths.

After feature extraction, the 12 3×3 outputs are flattened into a compact 72-bit vector, which serves as the input to a lightweight dense classifier. This classifier performs multiclass odor prediction across natural organic substances such as almond, broccoli, cloves, ginger, and kiwi. By utilizing a small 72-bit dense layer instead of a large fully connected network, the architecture minimizes the usage of registers, Lookup Tables (LUTs), and Block Random Access Memory (BRAM), thereby enabling efficient hardware deployment.

A. Odor Sensor Extraction

The odor identification pipeline begins with the acquisition of multi-channel gas sensor signals obtained from the SmellNet Herbal and Organic Dataset, which is available at the MIT Media Innovation Repository (https://github.com/MIT-MI/SmellNet) [14]. This dataset provides 12 sensing parameters for each odor sample from more than 50 categories. These parameters collectively form the chemical and environmental signature of organic substances such as almonds, broccoli, and so on. Each channel produces a time series of raw integer values representing the variation in sensor resistance or calibrated gas indices during odor exposure [27]. The parameters exhibit different signal amplitudes and dynamic ranges, as illustrated in Figure 1, where each channel produces an independent temporal curve [28].

To prepare the sensor data for CNN processing, a fixed number of 676 samples are reshaped into a two-dimensional grid array of 26×26, allowing the temporal signal to be represented as spatial texture. As shown in Figure 2, this transformation enables convolution filters with the support of the line buffer technique [23]. This proposed design achieves an efficient stride-1 convolution preprocessing method, which uses a line-buffer-based architecture to extract a 3×3 window from a 26×26 input for kernel multiplications without reloading the entire image into memory. Using the image convolution method, mapping is performed in a continuous 3×3 form,

which is segmented into three rows with three individual pixels each. The first row is given as (p0, p1, p2), the second row is given as (p3, p4, p5), and the third row is given as (p6, p7, p8). This technique efficiently reduces memory usage and ensures real-time pixel-wise processing with a single clock-cycle latency per shift.

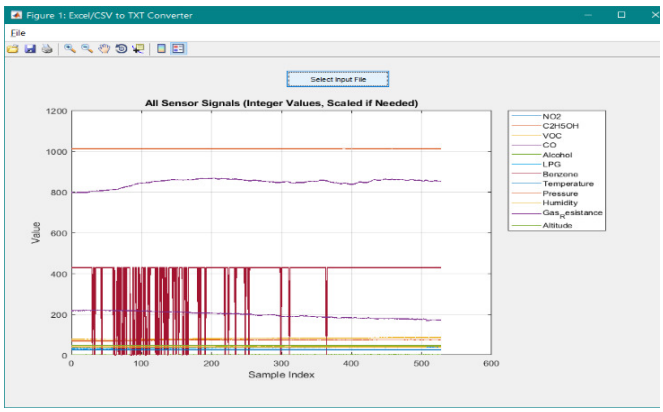

Fig. 1. Sensor samples of 26×26 window size from the dataset.

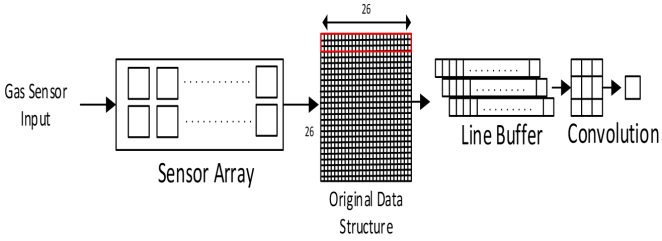

Fig. 2. Input data from the sensor array to convolution.

B. Depthwise and Pointwise Convolution with Rectified Linear Unit

Depthwise convolution and pointwise convolution are the core feature extraction components of the proposed odor classification network, and together they provide an efficient way to process each sensor channel without the heavy computational cost of standard convolution.

In the first stage, the depthwise convolution filter processes each gas sensor channel independently, allowing the network to capture local spatial variations in the 26×26 reshaped data structure. Furthermore, max-pooling is used to downsample the feature maps from 26×26 to 3×3, resulting in a compact 72-bit representation. This operation is important for each sensing parameter, such as NO_2, VOC, and humidity, which contribute unique and independent odor signatures that should not be mixed prematurely. In this way, computation is performed separately across 12 CNN processing branches. The combined depthwise and pointwise CNN architecture is shown in Figure 3.

By sliding a small 3×3 window across the 26×26 sensor matrix, each window position under stride-1 convolution is multiplied element-wise with the corresponding kernel coefficients. This multiplication is carried out in parallel using a fixed 3×3 multiplier array, where nine multipliers compute nine products at every clock cycle. These products are passed to an adder tree that sums them to produce a single filtered output value for each window position. Here, the line buffer plays a critical role in enabling this process; it shifts the data into three FIFO buffers and reads them simultaneously for multiplication. This reduces the number of memory operations and improves depthwise convolution efficiency on FPGA hardware. The sum of the nine products in the adder tree completes the depthwise convolution step for each pixel position and proceeds to the next stage of pointwise convolution.

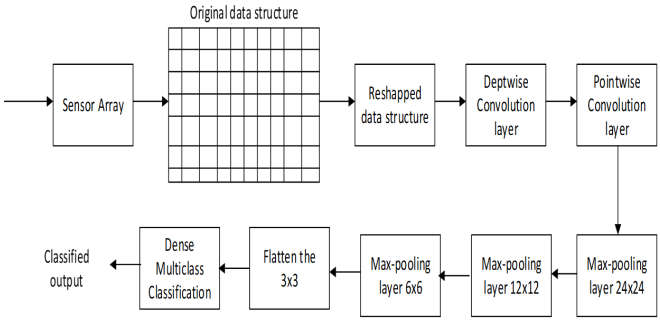

Fig. 3. CNN-based odor identification system architecture.

The mathematical operation of this depthwise filter per channel is given by:

$$Y_k(i,j) = \sum_{m=0}^{r-1}\sum_{n=0}^{r-1} X_k(i+m, j+n) D_k(m,n) \quad (1)$$

where $X_k \in \mathbb{R}^{H\times W}$ is the input of k-th sensor channel, $D_k \in \mathbb{R}^{r\times r}$ is the depthwise kernel for channel k, and $Y_k \in \mathbb{R}^{(H-r+1)\times(W-r+1)}$ is the output of depthwise convolution.

This depthwise convolution output is passed to the pointwise convolution in the second stage. It is responsible for combining the independent spatial features extracted by the depthwise convolution. The pointwise convolution performs channel-wise feature fusion using a 1×1 kernel across all input channels. It enables integration of channel information at each spatial position without changing spatial resolution. Even though the kernel size is small, it performs effective linear transformations at every pixel location.

Let the input feature map be:

$$X \in \mathbb{R}^{H\times W\times C} \quad (2)$$

where H is the height, W is the width, and C is the number of input channels.

Pointwise convolution transforms the input from C channels to C_{out} output channels using a 1×1×C kernel. Each output channel has its own weight vector and bias term.

For each spatial position (i,j), pointwise convolution is defined as:

$$P(i,j,c_{out}) = \sum_{k=1}^{C} X(i,j,k)W(k,c_{out}) + b_{c_{out}} \quad (3)$$

where $X(i,j,k)$ is the input feature value at location (i,j) in channel k, $W(k,c_{out})$ is the weight connecting input channel k to output channel c_{out}, b_{out} is the bias of the output channel, and $P(i,j,c_{out})$ is the output feature map.

The activation function is applied to introduce nonlinearity and improve training stability by mitigating gradient saturation. ReLU is defined as:

$$\text{ReLU}(x) = \max(0, x) \quad (4)$$

C. Operation of Max-Pooling for 6×6 to 3×3 Downsampling

Max-pooling is a downsampling operation used in CNNs to reduce the spatial size of a feature map while preserving the most dominant or representative values within each region. It operates by dividing the input feature map into non-overlapping windows and selecting the maximum value from each window [29]. This operation reduces computational complexity, lowers memory usage, and improves robustness to small spatial variations. Figure 4 illustrates an example of max-pooling using a 4×4 input mapped to a 2×2 and then to a 1×1 representation, where the pooling window slides across the feature map. At each step, the pooling operation extracts a local region, and the output corresponds to the maximum value within that region [30].

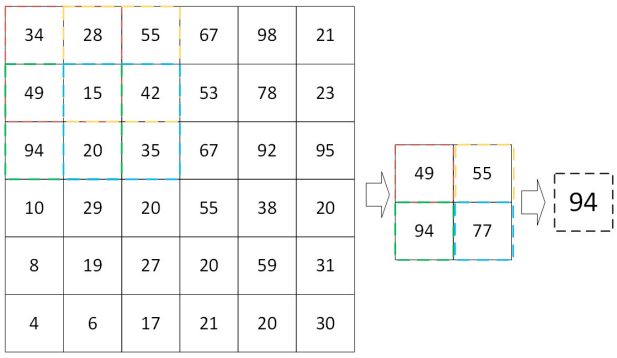

Fig. 4. Max-pooling operation from 3×3 to 1×1.

Let the input feature map be represented as:

$$X \in \mathbb{R}^{H \times W} \quad (5)$$

The output spatial dimensions after pooling are given by:

$$H' = \left|\frac{H-p}{s}\right| + 1, \; W' = \left|\frac{W-p}{s}\right| + 1 \quad (6)$$

where p is the pooling window size and s is the stride.

The max-pooling operation is defined as:

$$P(i,j) = \max\left\{X(i \cdot s + m, j \cdot s + n \mid 0 \le m < p, 0 \le n < p)\right\} \quad (7)$$

Figure 3 shows the CNN-based odor classification pipeline, which employs multiple max-pooling stages [31]. After pointwise convolution, max-pooling operations reduce the feature maps sequentially from 24×24 to 12×12, 12×12 to 6×6, and 6×6 to 3×3. The final 3×3 feature maps from all channels are flattened into nine 8-bit values. Considering 12 sensing channels processed in parallel, this results in a total feature representation of 72 bits, corresponding to 864 intermediate features. These values are then passed to the dense classification block [32], where learned weights map the compressed feature vector to the final odor class prediction.

In this odor classification system, each incoming sensor pattern and each stored trained sample are represented as a fixed-length binary feature vector of size N = 72 bits. This binary representation is obtained after preprocessing and feature extraction, enabling lightweight digital operations suitable for FPGA deployment. The 72-bit vector is passed to a Hamming distance-based comparator, which computes mismatches with stored training samples. The resulting distances are accumulated across each Hamming block to produce a final score for the 12 sensing inputs. This process is repeated for all categories, corresponding to 50 × 12 = 600 comparisons. The proposed pipelined architecture ensures deterministic and low-latency hardware computation, making it highly suitable for FPGA implementation.

III. RESULTS AND IMPLEMENTATION

The complete hardware implementation of the proposed odor identification system was developed using Verilog HDL, and the functional verification was performed in ModelSim. The design was synthesized on a Xilinx Artix-7 AC701 FPGA. A detailed comparison of hardware utilization between the proposed natural organic odor identification system and the herbal odor identification system reported in [17], developed using Chinese medicinal datasets, is provided in Table I.

TABLE I. COMPARISON ANALYSIS OF ODOR IDENTIFICATION SYSTEMS

Resource	**Odor identification of natural organic substance (This work)**	**Odor identification of Chinese herbal medicine dataset [17]**
FPGA	Artix-7 AC701	Arty z7-7020
LUT	34,664	53,200
FF	31,004	106,400
BRAM	138	630
Frequency (MHz)	100	100
Dataset	SmellNet Herbal and Organic Dataset	Chinese Medicinal Dataset
Total number of samples	700	8,000
Number of categories	7	50
Samples per category	100	12×676
Delay (ns)	4.146	8.924
Total power (W)	0.362	23.265

The proposed system required 34,664 LUTs, 31,004 Flip-Flops (FFs), and 13 BRAMs, whereas the reported design occupies 53,200 LUTs, 106,400 FFs, and 630 BRAMs. This analysis shows that the proposed architecture reduces resource consumption by approximately 34.8% in LUTs, 70.8% in FFs,

and 78.1% in BRAMs. These improvements clearly highlight the lightweight nature of the proposed system and its suitability for embedded platforms.

The power consumption of the proposed work is 0.362 W, making the design highly energy efficient for continuous odor monitoring applications. The system also achieves a latency of 4.146 ns, supporting low-latency inference compared to the larger existing method. Furthermore, Table II presents the resource utilization of the DWS-CNN, showing how each layer contributes to overall FPGA usage. The architecture includes image line buffering, depthwise convolution, pointwise convolution, and max-pooling layers, which collectively account for most logic utilization. The total utilization is 25.91% in LUTs, 0.62% in Look-Up Table-based Random Access Memory (LUTRAM), 11.59% in FFs, 37.81% in BRAM, and 3.13% in Global Clock Buffer (BUFG) relative to available FPGA resources. This low utilization indicates that the architecture still has sufficient logic capacity for extending odor categories, adding on-chip buffering, or integrating real-time wireless communication modules.

The timing performance of each processing block is summarized in Table III, and Figure 5 shows the functional verification of broccoli identification in ModelSim. The depthwise convolution requires 26.7 µs, the pointwise convolution requires 30.01 µs, and the max-pooling stages require 6.25 µs and 0.85 µs for the 12×12 and 6×6 stages, respectively. The dense multiclass classification with Hamming distance calculation completes its operation within 1.06 µs. Overall, the complete CNN model executes in 65.36 µs, which satisfies real-time constraints and is suitable for continuous odor detection applications. These timing results are well balanced in the hardware design, involving convolution and max-pooling stages.

TABLE II. RESOURCE UTILIZATION OF THE PROPOSED ODOR IDENTIFICATION DWS-CNN ARCHITECTURE

Type	LUT	LUTRAM	FF	BRAM	IO
Image line buffer	333	3	385	1.50	57
Depthwise convolution	350	69	35	1	100
ReLU	4	0	0	0	17
Pointwise convolution	12	0	21	0	31
Max-Pooling 24×24	619	7	742	3	39
Max-Pooling 12×12	619	7	694	3	35
Max-Pooling 6×6	566	7	756	3	91
DWS-CNN (total utilization)	34,664	288	31,004	138	250
FPGA available resources	133,800	46,200	267,600	365	400
Percentage (%)	25.91	0.62	11.59	37.81	62.50

TABLE III. TIMING ANALYSIS AND FUNCTIONAL VERIFICATION OF THE PROPOSED DWS-CNN MODEL

Layer	Type	Window size	Input size	Functional verification timing (µs)
Convolution	Depthwise convolution	3×3	26×26	26.7
	Pointwise convolution	1×1	24×24	30.01
	Max-pooling	6×6	12×12	6.25
	Max-pooling	6×6	6×6	0.85
Classification	Dense multiclass	3×3	72-bit	1.06
Total time	Proposed DWS-CNN model	26×26	26×26	65.36

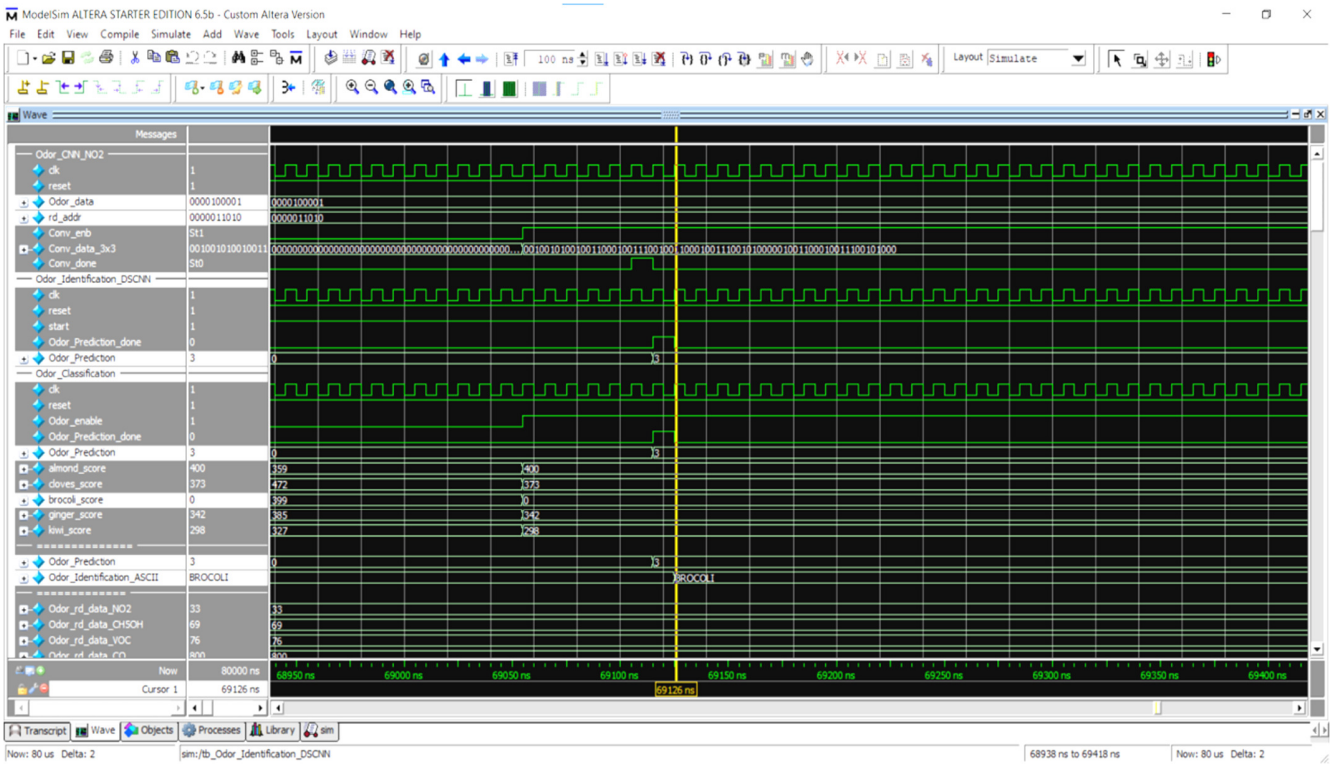

Fig. 5. Functional verification of broccoli identification in ModelSim.

IV. CONCLUSION

A lightweight Depthwise Separable Convolutional Neural Network (DWS-CNN) for odor identification was successfully designed and developed based on depthwise convolution and max-pooling-based downsampling methods, achieving an efficient, low-power odor classification system. This design is optimized to handle a minimum number of samples per second, enabling fast prediction of sensing results for real-time applications. This CNN-based classification accurately identifies herbal and organic substances across 50 categories, each described by 12 sensing values. The complete design was implemented on an Artix-7 FPGA, confirming the effectiveness of the experimental results. FPGA analysis significantly reduced the utilization of Look-Up Tables (LUTs), Flip-Flops (FFs), and Block Random Access Memory (BRAM) compared to the herbal odor identification system reported in [17], which is based on Chinese medicinal datasets.

Further, the integration of multiclass dense classification results in a lightweight architecture, which uses a 26×26 input structure and a flattened 8×8 representation for dense classification, ensuring balanced logic utilization, cost efficiency, and low power consumption. This approach is well suited for real-time odor analysis in herbal, medical, and chemical industry applications. Future work may include improving data security and robustness of classification, as well as incorporating the design into a wearable and portable platform with embedded wireless communication, supported by a System on Chip (SoC).

DECLARATION OF COMPETING INTERESTS

The authors declare that they have no known competing financial interests or personal relationships that could have appeared to influence the work reported in this paper.

ACKNOWLEDGMENT

The authors are grateful to the Government of India for the financial assistance provided through the National Fellowship Scheme and to the Gulbarga University.

DATA AVAILABILITY

The dataset used in this study is publicly available [14, 17, 33].

REFERENCES

[1] P. Singh, U. Habiba, Z. Shafi, A. Noor, V. K. Pandey, and R. Singh, "Understanding the Concepts of Smart E-Nose Technology in Combination With Machine Learning for New Era of Food Safety: An Advanced Review," *Food Safety and Health*, vol. 3, no. 4, pp. 518–534, Oct. 2025, https://doi.org/10.1002/fsh3.70029.

[2] F. R. Cavalcante *et al.*, "Determinants of Odor-Related Perception: Analysis of Community Response," *Atmosphere*, vol. 16, no. 10, Oct. 2025, Art. no. 1176, https://doi.org/10.3390/atmos16101176.

[3] S. Fuentes *et al.*, "Assessment of Smoke Contamination in Grapevine Berries and Taint in Wines Due to Bushfires Using a Low-Cost E-Nose and an Artificial Intelligence Approach," *Sensors*, vol. 20, no. 18, Sept. 2020, Art. no. 5108, https://doi.org/10.3390/s20185108.

[4] R. MacÃas-Quijas, R. VelÃ¡zquez, C. Del-Valle-Soto, R. Lizut, P. Visconti, and A. Lay-Ekuakille, "Environmental odor detection and classification with electronic nose system," *Bulletin of Electrical Engineering and Informatics*, vol. 14, no. 2, pp. 1117–1125, Apr. 2025, https://doi.org/10.11591/eei.v14i2.9046.

[5] H. Patel *et al.*, "Design Principles From Natural Olfaction for Electronic Noses," *Advanced Science*, vol. 12, no. 12, Mar. 2025, Art. no. 2412669, https://doi.org/10.1002/advs.202412669.

[6] E. L. Hines, E. Llobet, and J. W. Gardner, "Electronic noses: a review of signal processing techniques," *IEE Proceedings - Circuits, Devices and Systems*, vol. 146, no. 6, pp. 297–310, Dec. 1999, https://doi.org/10.1049/ip-cds:19990670.

[7] H. Wei and Y. Gu, "A Machine Learning Method for the Detection of Brown Core in the Chinese Pear Variety Huangguan Using a MOS-Based E-Nose," *Sensors*, vol. 20, no. 16, Aug. 2020, Art. no. 4499, https://doi.org/10.3390/s20164499.

[8] T. Sanislav, G. D. Mois, S. Zeadally, S. Folea, T. C. Radoni, and E. A. Al-Suhaimi, "A Comprehensive Review on Sensor-Based Electronic Nose for Food Quality and Safety," *Sensors*, vol. 25, no. 14, July 2025, Art. no. 4437, https://doi.org/10.3390/s25144437.

[9] J. Segura-Garcia *et al.*, "AI-driven 5G IoT e-nose for whiskey classification," *Applied Intelligence*, vol. 55, no. 10, Apr. 2025, Art. no. 686, https://doi.org/10.1007/s10489-025-06425-1.

[10] C. Cheng and K. K. Parhi, "Fast 2D Convolution Algorithms for Convolutional Neural Networks," *IEEE Transactions on Circuits and Systems I: Regular Papers*, vol. 67, no. 5, pp. 1678–1691, May 2020, https://doi.org/10.1109/TCSI.2020.2964748.

[11] J. Yepez and S.-B. Ko, "Stride 2 1-D, 2-D, and 3-D Winograd for Convolutional Neural Networks," *IEEE Transactions on Very Large Scale Integration (VLSI) Systems*, vol. 28, no. 4, pp. 853–863, Apr. 2020, https://doi.org/10.1109/TVLSI.2019.2961602.

[12] R. Handayani, R. Sarno, D. Rahman Wijaya, K. R. Sungkono, and D. Y. Kristiyanto, "An Approach Sensory Analysis Using Targeted Sensors in Electronic Nose for Assessing Green Tea Quality," in *2024 International Seminar on Intelligent Technology and Its Applications*, Mataram, Indonesia, 2024, pp. 746–751, https://doi.org/10.1109/ISITIA63062.2024.10667683.

[13] O. Sosa-Ramos *et al.*, "Study of the effect of relative humidity on the classification of volatile organic compounds for a quartz crystal microbalance sensors array," *Sensors and Actuators A: Physical*, vol. 387, June 2025, Art. no. 116465, https://doi.org/10.1016/j.sna.2025.116465.

[14] D. Feng, W. Dai, C. Li, A. Pernigo, and P. P. Liang, "SmellNet: A Large-scale Dataset for Real-world Smell Recognition," presented at the The Fourteenth International Conference on Learning Representations, Rio de Janeiro, Brazil, 2025, https://doi.org/10.48550/arXiv.2506.00239.

[15] R. L. Doty, "Odors as cognitive constructs: history of odor classification and attempts to map odor percepts to physical and chemical parameters," *Chemical Senses*, vol. 50, Jan. 2025, Art. no. bjaf022, https://doi.org/10.1093/chemse/bjaf022.

[16] M. H.-M. Khan *et al.*, "Multi- class classification of breast cancer abnormalities using Deep Convolutional Neural Network (CNN)," *PLOS ONE*, vol. 16, no. 8, Aug. 2021, Art. no. e0256500, https://doi.org/10.1371/journal.pone.0256500.

[17] Z. Mo, D. Luo, T. Wen, Y. Cheng, and X. Li, "FPGA Implementation for Odor Identification with Depthwise Separable Convolutional Neural Network," *Sensors*, vol. 21, no. 3, Jan. 2021, Art. no. 832, https://doi.org/10.3390/s21030832.

[18] D. L. T. Wong, Y. Li, D. John, W. K. Ho, and C. H. Heng, "Resource and Energy Efficient Implementation of ECG Classifier Using Binarized CNN for Edge AI Devices," in *2021 IEEE International Symposium on Circuits and Systems (ISCAS)*, Daegu, Korea, 2021, pp. 1–5, https://doi.org/10.1109/ISCAS51556.2021.9401427.

[19] L. Bai, Y. Zhao, and X. Huang, "A CNN Accelerator on FPGA Using Depthwise Separable Convolution," *IEEE Transactions on Circuits and Systems II: Express Briefs*, vol. 65, no. 10, pp. 1415–1419, Oct. 2018, https://doi.org/10.1109/TCSII.2018.2865896.

[20] I. Yuadi, N. U. Nazikhah, C.-C. Hu, K. Nisa', and V. S. Suryakala, "Deep Learning-Based Galls and Healthy Leaf Recognition Using Depthwise Separable CNN Architecture," *Engineering, Technology &*

Applied Science Research, vol. 15, no. 3, pp. 23777–23782, June 2025, https://doi.org/10.48084/etasr.11142.

[21] D. R. Wijaya, R. Handayani, M. D. Badri, S. Shabri, and V. P. Rahadi, "Data set for Gambung green tea aroma using on electronic nose," *BMC Research Notes*, vol. 17, no. 1, Sept. 2024, Art. no. 244, https://doi.org/10.1186/s13104-024-06905-6.

[22] D. Ameta, S. Kumar, R. Mishra, L. Behera, A. Chakraborty, and T. Sandhan, "Odor classification: Exploring feature performance and imbalanced data learning techniques," *PLOS ONE*, vol. 20, no. 5, May 2025, Art. no. e0322514, https://doi.org/10.1371/journal.pone.0322514.

[23] X. Chen, J. Ji, S. Mei, Y. Zhang, M. Han, and Q. Du, "FPGA Based Implementation of Convolutional Neural Network for Hyperspectral Classification," in *IGARSS 2018 - 2018 IEEE International Geoscience and Remote Sensing Symposium*, Valencia, Spain, 2018, pp. 2451–2454, https://doi.org/10.1109/IGARSS.2018.8517973.

[24] X. Zhao *et al.*, "HDSuper: High-Quality and High Computational Utilization Edge Super-Resolution Accelerator With Hardware-Algorithm Co-Design Techniques," *IEEE Transactions on Circuits and Systems I: Regular Papers*, vol. 71, no. 4, pp. 1679–1692, Apr. 2024, https://doi.org/10.1109/TCSI.2024.3354125.

[25] W. Li, H. Leung, C. Kwan, and B. R. Linnell, "E-Nose Vapor Identification Based on Dempster–Shafer Fusion of Multiple Classifiers," *IEEE Transactions on Instrumentation and Measurement*, vol. 57, no. 10, pp. 2273–2282, Oct. 2008, https://doi.org/10.1109/TIM.2008.922092.

[26] D. Wu, D. Luo, K.-Y. Wong, and K. Hung, "POP-CNN: Predicting Odor Pleasantness With Convolutional Neural Network," *IEEE Sensors Journal*, vol. 19, no. 23, pp. 11337–11345, Dec. 2019, https://doi.org/10.1109/JSEN.2019.2933692.

[27] H. Nishijima *et al.*, "Optimizing Odorants for Olfactory Training Based on Olfactory Receptor–Ligand Pair Analysis," *The Laryngoscope*, vol. 136, no. 1, pp. 384–394, Jan. 2026, https://doi.org/10.1002/lary.32437.

[28] I. Shtepliuk, K. Montelius, J. Eriksson, and D. Puglisi, "Adaptive Machine Learning for Electronic Nose-Based Forensic VOC Classification," *Advanced Science*, vol. 12, no. 36, Sept. 2025, Art. no. e04657, https://doi.org/10.1002/advs.202504657.

[29] A. M. Dhanush Gowda, A. D. Dessai, and U. Y. Nayak, "Electronic-Nose Technology for Lung Cancer Detection: A Non-Invasive Diagnostic Revolution," *Lung*, vol. 203, no. 1, July 2025, Art. no. 76, https://doi.org/10.1007/s00408-025-00828-0.

[30] Y. Zhou, J. Wang, and S. Zhou, "A Dense Network Model of Traffic Classification Based on Autoencoder and Attention Mechanism," in *2024 IEEE 12th International Conference on Computer Science and Network Technology*, Dalian, China, 2024, pp. 55–59, https://doi.org/10.1109/ICCSNT62291.2024.10776636.

[31] H. Zhang, H. Yu, Z. Xu, K. Zheng, and L. Gao, "A Novel Classification Framework for Hyperspectral Image Classification Based on Multi-Scale Dense Network," in *2021 IEEE International Geoscience and Remote Sensing Symposium IGARSS*, Brussels, Belgium, 2021, pp. 2238–2241, https://doi.org/10.1109/IGARSS47720.2021.9555010.

[32] Y. Zhou, S. Zhou, and J. Cui, "An Encrypted Traffic Classification Model Based on Improved Dense Network and Bidirectional Gated Recurrent Unit," in *2024 IEEE 12th International Conference on Computer Science and Network Technology*, Dalian, China, 2024, pp. 60–66, https://doi.org/10.1109/ICCSNT62291.2024.10776672.

[33] D. Feng, "MIT-MI/SmellNet." MIT Multisensory Intelligence Group, Apr. 22, 2026, [Online]. Available: https://github.com/MIT-MI/SmellNet.

AUTHORS PROFILE

Akshata K. Aldi received the B.E. degree in Electronics and Communication Engineering and M.Tech degree in VLSI and Embedded Systems. She is currently pursuing a Ph.D. in Applied Electronics. She has Qualified GATE, UGC-NET, and K-SET examinations. Her research interests include FPGA-based systems, VLSI design, embedded systems, AI-based architectures, and electronic nose technology.

R. L. Raibagkar is currently a Senior Professor and Chairman at Department of P.G. studies and research in Applied Electronics, Gulbarga University. His research interests include electronic perovskite ceramic materials, material synthesis and characterization, IoT-based systems, semiconductor electronics, and microelectronics. He has extensive expertise in materials science, electronic engineering, and embedded electronic systems.